A Detailed Investigation of the Transitional Boundary Layer on the Suction Side of a Turbine Blade

Ugo Campora, Ferruccio Pittaluga, Marina Ubaldi, Pietro Zunino
Dipartimento di Macchine, Sistemi Energetici e Trasporti
Università di Genova, Italy

ABSTRACT

An extensive data base concerning the boundary layer transition on the suction side of a large-scale turbine blade arranged in linear cascade has been made available at the internet address <http://transition.imse.unige.it/cases/Goa>.

Boundary layer velocity measurements were performed by means of a two-component fibre optic laser Doppler velocimeter.

The paper reports on the experimental difficulties encountered in the near wall measurements and gives a detailed description of the data processing procedures which apply to instantaneous LDV velocity data, in order to investigate the boundary layer transition process.

NOMENCLATURE

C_f wall friction coefficient
c blade chord length
f frequency
g cascade pitch
H_{12} shape factor $= d^* / q$
Re_{2c} Reynolds number based on cascade outlet velocity and chord length $= u_2 c / \nu$
Re_q momentum thickness Reynolds number $= u_e \theta / \nu$
S spectral density
S_k skewness coefficient
s surface distance measured from leading edge
$s_{\max}$ surface length from leading to trailing edge
T_l integral time scale
Tu free-stream turbulence intensity
t time
u, v instantaneous velocity components in streamwise and cross-stream directions
u', v' velocity fluctuations in streamwise and cross-stream directions
u_e local free-stream velocity
u_t wall friction velocity $= \sqrt{t_w / r}$
u^+ dimensionless velocity $= \bar{u} / u_\tau$
y normal distance from the wall
y^+ dimensionless distance from the wall $= y u_t / n$

d^* boundary layer displacement thickness
q boundary layer momentum thickness
ν kinematic viscosity
ρ fluid density
t_w wall shear stress

Subscripts
1   cascade inlet
2   cascade outlet

Overbar
——   time averaged

1. INTRODUCTION

Accurate numerical prediction of the transitional boundary layer on turbomachinery blades is still a not completely resolved issue. Overestimation of turbulence production in impinging leading-edge flows is a particularly serious problem that provokes too early transition prediction and underestimation of the transition length [1]. Therefore, detailed experimental data specially produced for turbulence model assessment purpose, such as Reynolds stress and turbulence production term distributions, are of primary importance for improving transition model predictive capabilities.

With this view, few years ago, an extensive database concerning the transitional boundary layer development at high Reynolds number on the suction side of a gas turbine vane was experimentally produced by the present authors [2]. This database, recently adopted as official test case by the ERCOFTAC Transition Modelling SIG10 and TRANSPRE-TURB (European Thematic Network on Implementation and Further Application of Refined Transition Prediction Methods for Turbomachinery), is being widely employed by research groups operating in turbulence and transition modelling [3, 4, 5].

With the aim of studying the effect of Reynolds number on the blade boundary layer transition, a new experimental investigation has been recently undertaken on the same geometry at lower Reynolds numbers. The use of a more advanced LDV instrumentation and the thickening of the linear sublayer, due to the Reynolds number reduction, resulted in higher degree of spatial resolution of measurements and improved accuracy of results.

Two data bases, the previous one at $\mathrm{Re}_{2c} = 1600000$ and a new one at $\mathrm{Re}_{2c} = 590000$ are now available at the internet address <http://transition.imse.unige.it/cases/Goa>.

The present paper reports on the experimental difficulties encountered in near-wall velocity LDV measurements and focuses on the data processing procedures applied to the instantaneous LDV data to investigate boundary layer transition.

2. EXPERIMENTAL SETUP

2.1 Test Facility

The blade boundary layer development was surveyed on the suction side of the central blade of a three-blade large-scale linear turbine cascade installed in the low-speed wind tunnel of DIMSET. The facility is a blow-down continuously operating variable speed wind tunnel with an open test section of 500x300 mm^2. A three-blade cascade with the largest possible blade chord was used so as to maximise measurement spatial resolution.

The blade profile is representative of a coolable hp gas turbine nozzle blade and is the same tested during an European project on time-varying wake flow characteristics on flat plates and turbine cascades [6]. Coordinates of the profile are given in [7].

The relevant geometrical characteristics of the cascade are: chord length $c = 300$ mm, pitch-to-chord ratio $g/c = 0.7$, blade aspect ratio $h/c = 1$, gauging angle $\boldsymbol{b_2}' = 19.2°$.

2.2 Instrumentation

A two-colour fibre optic LDV system with backscatter collection optics (Dantec Fiber Flow) is the main instrument for the present investigation. The light source is a 300 mW argon ion laser operating at 488 nm (blue) and 514.5 nm (green).

The probe consists of an optical transducer head of 60 mm diameter connected to the emitting optics and to the photomultipliers by means of optic fibres. The probe volume of 47 μm diameter and 0.4 mm length contains two sets of blue and green fringes (with spacing of 2.1 μm and 2.2 μm, respectively), which allow the simultaneous measurement of two velocity components in the plane perpendicular to the probe optical axis. A Bragg cell is used to apply a frequency shift (40 MHz) to one of each pair of beams, providing directional sensitivity and reducing angle bias for all velocity measurements. The signals from the photomultipliers are processed by two Enhanced Burst Spectrum Analysers.

2.3 Test conditions and experiment organisation

The suction side boundary layer was surveyed at the Reynolds number based on the blade chord $\mathrm{Re}_{2c} = 590000$. The upstream turbulence level based on the streamwise velocity fluctuations and the outlet velocity was about 1.5 %. Information on the decay of the free-stream turbulence kinetic energy along the turbine blade is available.

The probe volume was oriented with the larger dimension along the spanwise direction in order to have better spatial resolution in the wall normal direction. In order to measure simultaneously streamwise and normal velocities close to the blade surface, the optical axis was tilted towards the wall of about half the angle of the intersecting beams.

The probe was traversed using a three-axis computer controlled probe traversing system. The motion was transmitted to the carriages by stepping motors through a pre-loaded ball-screw assembly, with a minimum linear translation step of 8 μm.
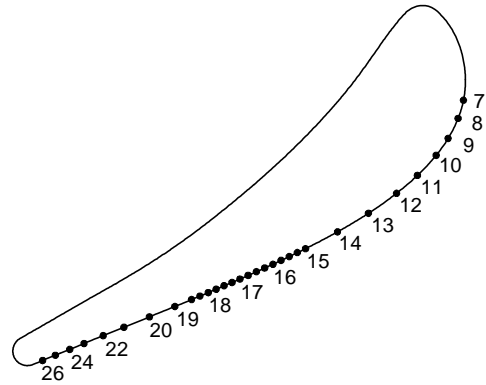

Fig. 1. Blade profile and boundary layer traverses location.

The flow was seeded with a 0.5-2 μm atomised spray of mineral oil injected in the flow at about 2 chord upstream of the cascade leading edge.

The boundary layer was surveyed by means of 31 traverses normal to the blade surface at midspan. The location of the boundary layer traverses and their corresponding reference numbers are shown in Fig. 1. Each boundary layer traverse is constituted by 34 measuring points. The distance between adjacent points was set at 25 μm in the region of the boundary layer close to the wall and was progressively increased in the outer part. The first point was set at a distance of 25 μm from the estimated wall position.

The measurements of the two velocity components were made in coincidence mode. Typical data rate was 10 kHz falling off to few kHz in the inner part of the boundary layer. For each measuring point 30000 samples were collected to obtain accurate statistical moments.

3. NEAR WALL MEASURING PROBLEMS

The friction velocity $u_\tau = \sqrt{\tau_w / \rho}$ is a quantity of prime importance for the characterisation of a boundary layer, especially for identifying transition or separation conditions and for evaluating boundary layer loss production. In principle, u_τ may be determined from mean velocity data in two different ways (e. g. Durst et al. [8]). Assuming that an analytical law for the velocity profile holds (for instance the log-law for turbulent boundary layers), one can extrapolate the velocity gradient at the wall employing velocity values measured even far from the wall. Otherwise, provided that velocity has been measured in a sufficient number of points within the linear sublayer ($y^+ \leq 5$), one can directly calculate $\left(\partial u / \partial y \right)_w$ from the experimental results (wall slope method) $u_\tau = \sqrt{\nu \left(\partial u / \partial y \right)_w}$. The first method is suitable for laminar and turbulent boundary layers, where the analytical law of the velocity profile is known, but cannot be used for transitional boundary layers. In this case it is necessary to set some measuring points in the linear sublayer region (one point is not enough due to the uncertainty in the identification of the wall position). Since the thickness of the linear sublayer region is very small and decreases as the Reynolds number increases, it can happen that at very high Reynolds numbers the wall-slope method fails to work, because no data can be obtained in the linear velocity region. Therefore, the possibility of measuring the friction velocity from the mean velocity profile in a transitional boundary layer depends on Reynolds number, probe volume dimension, minimum distance among points, uncertainty in wall position estimation.

In order to determine the wall position, during the approach of the probe volume to the wall, the photomultiplier signal was observed on an oscilloscope. The wall position has been assumed to correspond to the point of maximum light reflection from the wall. With a probe volume diameter $d = 47$ μm, at a distance of 25 μm from the wall, nominally there is no interference between the wall and the probe volume. Accordingly to the technical literature, the uncertainty in the wall position can be estimated in $e_y = \pm\, 0.3 \div 0.4\, d$, that means $\pm\, 14\text{-}19$ μm. In the present experiment the error never exceeded ± 16 μm, value that corresponds to twice the minimum step of the traversing system and thus the interference with the wall was always below $0.35\, d$. Assuming a value of 0.8 m/s for the friction velocity, u_t in the transitional region, the probe volume diameter is expressed in wall coordinates as $d^+ = d\,u_t\,/\boldsymbol{n} = 2.5$ and the uncertainty in determining the wall position is $\varepsilon_y^{\,+} = \varepsilon_y\, u_\tau\,/\nu = \pm 0.85$.

In the near wall region measuring steps of $\Delta y = 25$ μm were adopted, which correspond to $\Delta y^+ = 1.3$. In this way at least 3 measuring points are positioned within the laminar sublayer ($y^+ \leq 5$) giving enough confidence in applying the linear regression to the experimental data.

In regions of large velocity gradients, there is a particularly serious problem with the rms value of the streamwise velocity fluctuations, due to the finite dimension of the probe volume: the spatial velocity variations through the probe volume are interpreted by the instrument as fluctuations in time. Therefore, in the viscous sublayer, due to the large velocity gradients in the direction normal to the wall, the rms values of the streamwise velocity fluctuations are overestimated. The error in the rms u' value due to the finite dimensions of the probe volume may be evaluated by means of the expression $\Delta u' \cong (d\,/\,4)\,\P\,\overline{u}\,/\,\P\,y$ [9, 10]. Since in the laminar sublayer the velocity profile is linear $u^+ = y^+$, one gets $\Delta u'^+ \cong d^+\,/\,4$ and in the present case it is $\Delta u'^+ \cong 0.62$. This result suggests that in the laminar sublayer the rms u' will be overestimated of a factor $0.62\, u_t$ which, considering the low turbulence level in this region, corresponds to an error of the order of 100%. However, as the distance from the wall increases, the error in the rms of the streamwise velocity rapidly becomes negligible, due to the reduction of the velocity gradient and the simultaneous increase of turbulence intensity.
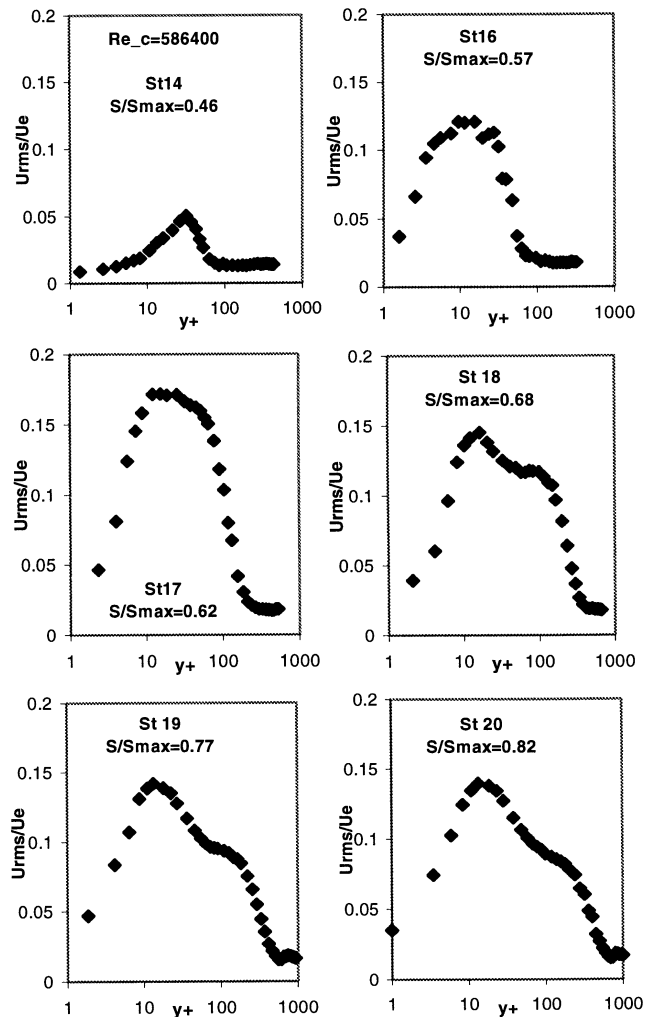

Fig. 2. Boundary layer mean velocity profiles in inner-law variables.

Fig. 3. Streamwise turbulence intensity profiles.

4.   DATA PROCESSING PROCEDURES

Scope of the present section is exemplifying the data processing procedures that can be applied to the instantaneous LDV realisations to get insight into the boundary layer transition process:
- statistical moments and probability density functions;
- time traces of the instantaneous velocity and power density spectra;
- boundary layer integral parameters.

4.1 Statistical moments and probability density function

In order to avoid statistical bias in the evaluation of the statistical moments for highly turbulent flows, transit time weighted averages have been applied to the LDV realisations:

- mean velocity $\overline{u} = \sum_{i=1}^{I} u_i \Delta t_i \left/ \sum_{i=1}^{I} \Delta t_i \right.$

- standard deviation of the velocity fluctuations

$$u_{rms} = \left(\sum_{i=1}^{I} (u_i - \overline{u})^2 \Delta t_i \left/ \sum_{i=1}^{I} \Delta t_i \right. \right)^{1/2}$$

- cross moment $\overline{u'v'} = \sum_{i=1}^{I} (u_i - \overline{u})(v_i - \overline{v}) \Delta t_i \left/ \sum_{i=1}^{I} \Delta t_i \right.$

- skewness coefficient $S_k = \sum_{i=1}^{I} (u_i - \overline{u})^3 \Delta t_i \left/ u_{rms}^3 \sum_{i=1}^{I} \Delta t_i \right.$

Since in the inner region the boundary layer is governed by viscous effects, inner layer variables $u^+ = \overline{u}/u_t$ and $y^+ = yu_t/\textbf{\textit{n}}$ are the most suitable coordinates for a careful evaluation of velocity and turbulence profiles.

Velocity profiles can be compared with well established semi-empirical correlations for turbulent boundary layers (e.g. White [11]):
- the linear correlation in the viscous sublayer range $y^+ \leq 5$

$u^+ = y^+$

- the law of the wall in the overlap layer range $35 \leq y^+ \leq 350$

$$u^+ = \frac{1}{k} \ln y^+ + B$$

with $k = 0.41$ and $B = 5$.

Data fitting against analytical relationships allows to evaluate possible errors in wall location, calculate wall friction velocity, as explained in section 3, and identify if the boundary layer at that station is in laminar, turbulent or transitional regime.

An example of mean velocity profiles, showing the boundary layer development from laminar to turbulent through transitional conditions, is given in Fig. 2. Velocity profiles are laminar like until station 16 ($s/s_{max} = 0.57$), where the experimental data fit a large portion of the curve $u^+ = y^+$, they are transitional at station 17 and 18 ($s/s_{max} = 0.62$ and 0.68) and evolve to fully turbulent log-law profiles from station 19 ($s/s_{max} = 0.77$).

Figure 3 shows the rms values of the streamwise velocity fluctuations at the same stations of Fig. 2. Surprisingly, at station 16, unless a laminar-like mean velocity profile is evident, streamwise velocity fluctuations are strongly amplified, showing that the transition process is already begun. In the laminar regime the maximum of the rms distribution is located at $y^+=30$. In the transition the peak becomes larger
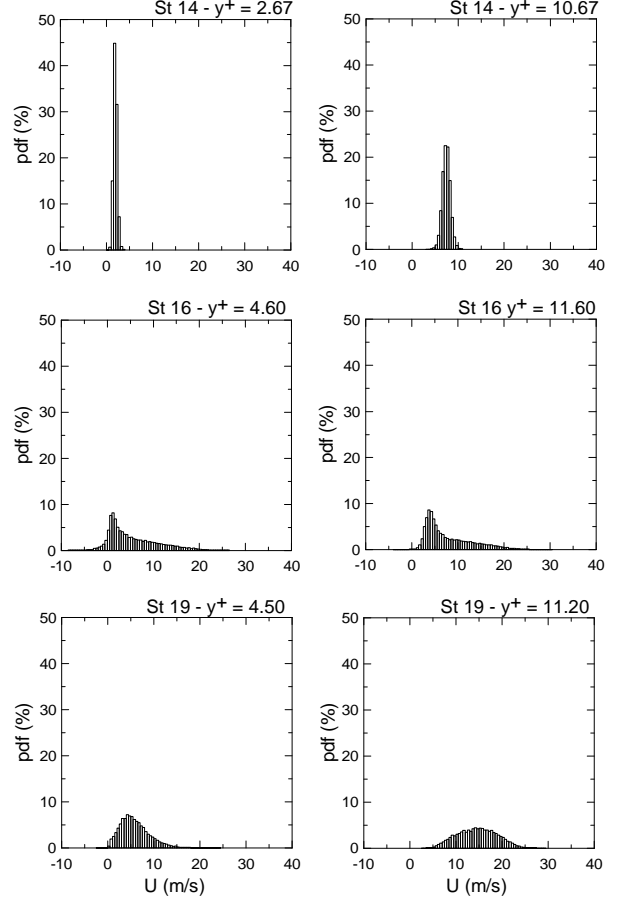

Fig. 4. Probability density functions of the streamwise velocity within the boundary layer: laminar (st. 14), transitional (st. 16), turbulent (st. 19).

than 18 per cent of the free-stream velocity and moves towards the wall. In the later stage of transition, the peak drops down to 15 per cent and a second characteristic hump appears beyond $y^+= 100$. At station 20 the distribution has become typical of turbulent boundary layers [12].

Probability density function (pdf) helps to interpret the shape of the velocity signal even in case of low data density. The discrepancy at station 16 between the laminar like velocity profile and the increase of streamwise velocity fluctuations, for instance, can be explained by pdf.

Figure 4 compares pdf of streamwise velocity at station 16 in the near wall region ($y^+= 4.6$ and 11.6) with pdf taken at corresponding positions of laminar (station 14, $y^+= 2.7$ and 10.7) and turbulent profiles (station 19, $y^+= 4.5$ and 11.2).

In the laminar region pdf show narrow-band Gaussian shape with low values for the mean. In turbulent regime, at approximately the same y^+, pdf show large-band Gaussian distributions with larger mean values. On the contrary, at station 16, pdf show long positive tails revealing that the rms rise is due to not so frequent large positive velocity spikes associated to turbulence spot passages, rather than nearly symmetrical turbulence fluctuations. The same pdf show also the presence of rare negative velocities, indicating that an incipient separation is going to initiate, but the process is inhibited by the taking place of the transition. It happens that, in contrast to the large standard deviation of the samples, the mean value remains low in agreement with laminar-like velocity profiles. This shows also that the steep increase of rms streamwise velocity fluctuations or the abrupt positive shift of the skewness coefficient [13, 14] are more efficient
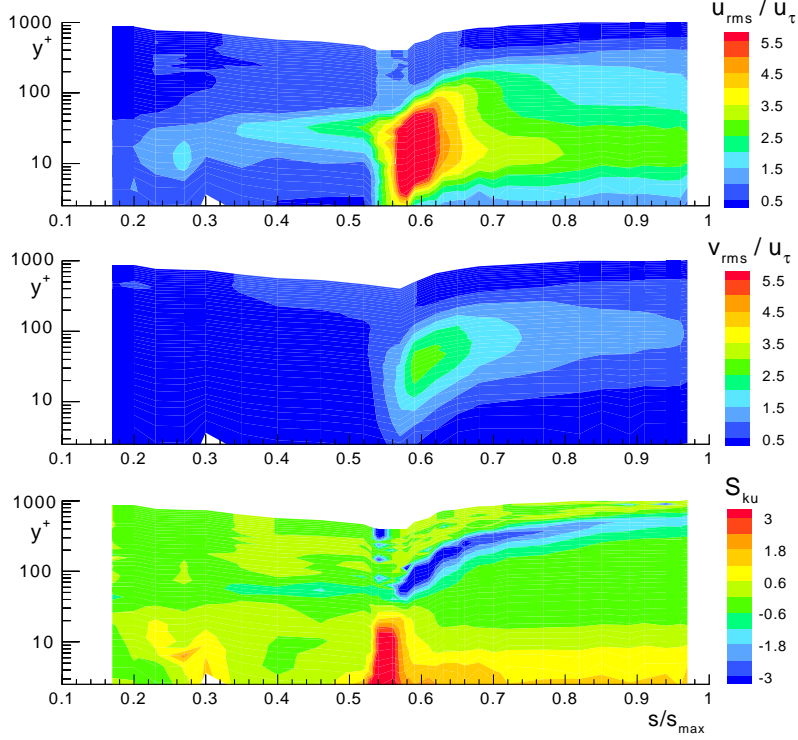
Fig. 5. Standard deviations and skewness coefficient in the boundary layer.

indicators of the departure from laminar conditions than the change of shape of velocity profiles.

This concept is clearly exemplified by the colour plots of Fig. 5 showing the distributions of the standard deviations of the velocity fluctuations in streamwise and cross-wise directions and the skewness coefficient as a function of the non-dimensional streamwise coordinate s/s_{max} and non-dimensional distance from the wall y^+. Both second and third order statistical moments of the streamwise velocity clearly indicate the onset of transition at $s/s_{max} = 0.53$. Contour plots also indicate that the transition process takes place mainly in the region below y^+=20. Comparison between the rms of the two velocity components shows also the strong anisotropy of the velocity fluctuations in the transition and in the turbulent boundary layer.

4.2 Time traces of the velocity and power spectral density

A measure of LDV capability in following the flow-velocity time-variations is given by the mean data density N_D, defined as the ratio between the integral time scale T_l and the mean valid data interarrival time Δt_s (the inverse of validated data rate):

$$N_D = T_l / \Delta t_s$$

The integral time scale T_l represents the period of the fluctuations associated with the largest flow structures.

Values of N_D of the order of 50 or larger are sufficient to provide a signal looking like a continuous representation of the velocity time history which allows a detailed description of the fine structure of the flow [15]. In the present investigation, the maximum obtainable data density is of the order of 20, a value that is not sufficient for the identification of the smallest flow fluctuations, but is large enough to reveal the general features of the time structure of the flow.

As an example Fig. 6 compares the time-series of measuring points of station 16 (in the transition region) with those of the corresponding points, at approximately the same y^+, of station 19 (in the turbulent region).
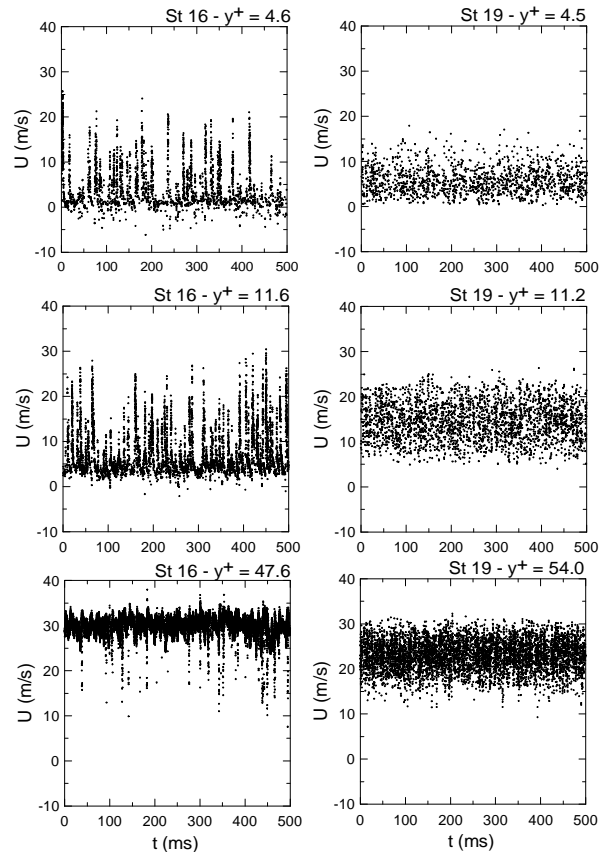

Fig. 6. Velocity time series within the boundary layer.

The most striking feature of the velocity traces of station 16 is the presence of not so frequent one-side velocity fluctuations, which determines the intermittent switching of the velocity from laminar to turbulent conditions. At $y^+ = 4.6$ time trace shows also some negative velocity values, indicating the tendency of the boundary layer to separate.

At station 19, the turbulence structure is characterised by higher frequency two-side large velocity fluctuations.

Power spectral density offers a means to evaluate the energy distribution across the frequency range characteristic of the flow time-varying structure. The two-sided spectral density function of the streamwise fluctuations (S_{uu}) can be evaluated from the direct Fourier transform of the velocity fluctuations.

$$S_{uu}(f) = \lim_{T \to \infty} \frac{1}{T} \left| \int_0^T u'(t) e^{-i2\pi ft} dt \right|^2 \qquad (1)$$

and $\displaystyle \int_{-\infty}^{+\infty} S_{uu}(f) df = \overline{u'^2}$

Furthermore quantities relevant for the statistical theory of turbulence, such as the integral time scale T_l and the Taylor time microscale T_l can be directly evaluated from the spectral density function [16]. The integral time scale T_l is given by the following relationship:

$$T_l = \frac{1}{\overline{u'^2}} \int_0^\infty C_{uu}(t) dt = \frac{S_{uu}(0)}{2\overline{u'^2}} \qquad (2)$$

where $C_{uu}(t)$ is the autocovariance function

$$C_{uu}(t) = \lim_{T \to \infty} \frac{1}{T} \int_0^T u'(t) u'(t+t) dt$$

and $\qquad S_{uu}(f) = \int_{-\infty}^\infty C_{uu}(t) e^{-i2\pi ft} dt$

As opposed to instrumentation which provides continuous signals, due to the discontinuous and random transit of particles in the measurement volume, the LDV output is a discrete and non-equispaced time series. In order to perform the spectral analysis, it is necessary to reconstruct an equispaced signal. The technique adopted in the present analysis is the sample and hold technique with multisample interpolation. A defect of this procedure is the production of a filtering noise acting like a low-pass filter [17], which attenuates the spectrum at frequencies larger than $\dot{n}/2\pi$, where $\dot{n}$ is the mean data rate.

If we consider a typical data rate for the present analysis of 10 kHz, the maximum unaffected range is 1600 Hz. As a consequence the resulting spectral density distribution may be not sufficiently accurate for the evaluation of quantities like the turbulence dissipation rate ε and the related small scales, but it is adequate for determining the time integral scale directly from eq. 2. In the present investigation the integral scale within the boundary layer varies from 0.5 ms to 2 ms.

Figure 7 compares the power spectra for points located at approximately the same non-dimensional distance from the wall ($y^+ \cong 4.5$ and 11) in transitional and turbulence traverses (stations 16 and 19, respectively).

The main difference between the two spectral distributions is the characteristic increase during transition of the spectral density in the low-frequency range (below 300 Hz) which is indicative of the broad band velocity fluctuations associated with the intermittent character of transition. For the turbulent condition, on the contrary, the spectral density increases in the higher frequency range.
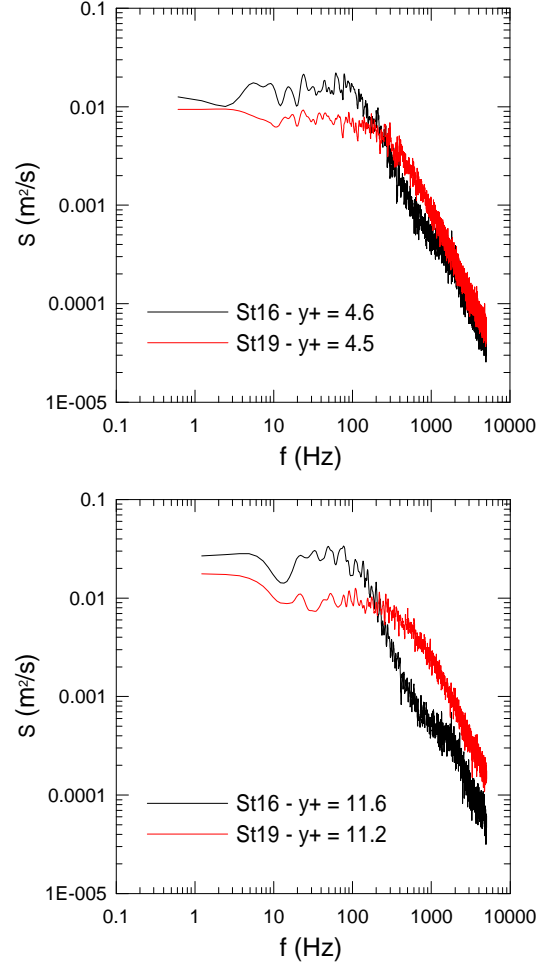

Fig. 7. Power density spectra of the streamwise velocity within the boundary layer.

4.3 Boundary layer integral parameters

Integral parameters provide global information essential for a practical evaluation of the boundary layer development such as flow blockage, energy losses and wall friction force. Integral parameter distributions are also sensitive indicators for identifying the boundary layer nature, the beginning and end of transition. Experimental-numerical comparisons are very often based on integral parameters and many transition correlations include such quantities.

Integral parameters are evaluated by direct numerical integration of the experimental velocity profiles. Wall friction coefficient depending on u_t / u_e is evaluated by data fitting against the curve $u^+ = y^+$ in the linear sublayer, as explained in section 3.

$$\delta^* = \int_0^\delta (1 - \overline{u}/u_e)\, dy$$

$$\vartheta = \int_0^\delta (1 - \overline{u}/u_e)\, \overline{u}/u_e\, dy$$

$$H_{12} = \delta^* / \vartheta$$

$$\mathrm{Re}_\vartheta = \vartheta u_e / \nu$$

$$C_f = 2\tau_w / (\rho u_e^2) = 2\,(u_t / u_e)^2$$

Figure 8 compares the distributions of the integral parameters for the two experiments carried out at
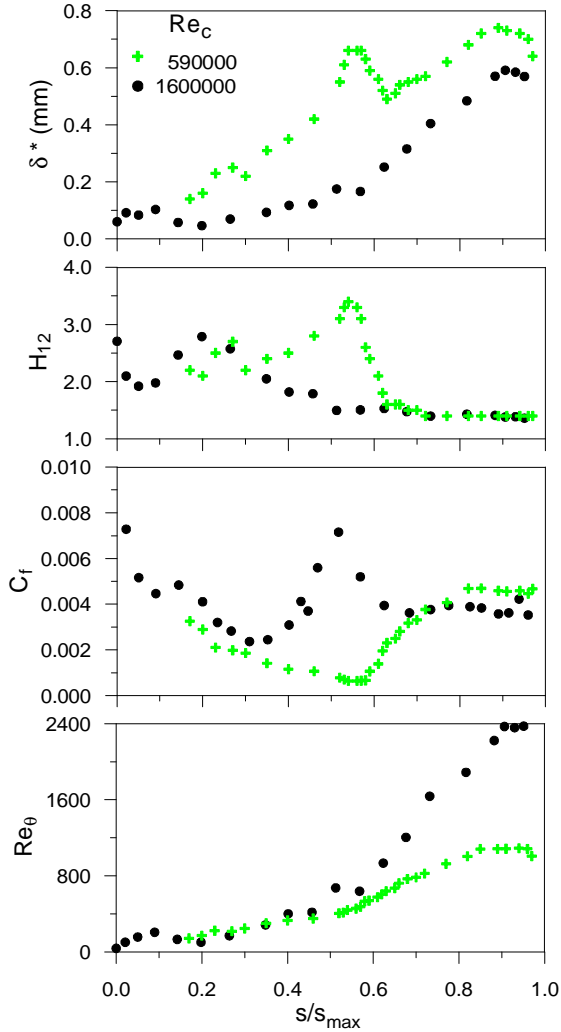
Fig. 8. Boundary layer integral parameters.

The distributions of Re_q substantially support the Mayle [19] and Hourmouziades [20] relationships, which for the present experiments give respectively:

$$\text{Re}_{qt} = 400 \; Tu^{-5/8} = 310$$

$$\text{Re}_{qt} = 460 \; Tu^{-0.65} = 353$$

However, for the present experiments, due to the moderate increase of Re_q in the early stage of transition, this parameter appears not very suitable from a practical point of view for identifying the beginning of transition.

CONCLUSIONS

Due to its inherent non-intrusive characteristics, capability to resolve directional ambiguity and wall heat-conduction insensibility, LDV is, in principle, an instrument well suited for investigating boundary layer flows.

In practice, however, the use of LDV in near wall measurements is not straightforward mainly because of the probe volume finite dimensions effects and the non-continuous random character of LDV output. In order to obtain reliable results, careful evaluation of limitations, problems and uncertainties associated with the above shortcomings are essential. Such issue has been widely discussed in the present paper.

Making reference to an experimental investigation of the suction side profile boundary layer on a large scale turbine blade, the data processing techniques applied to the LDV velocity realisations in order to extract complementary information on the transition process have been discussed in details and exemplified. At the moderate chord Reynolds number of the experiment $\text{Re}_{2c} = 590000$, the experimental procedures and the data processing techniques proved to be adequate for an accurate description of the boundary layer development and for producing detailed reliable data about the transition process, suitable for comparisons and assessment of transition predictive tools.

ACKNOWLEDGEMENTS

REFERENCES

[1] Leschziner, M. A., 1998, "Turbulence Modeling for Physically Complex Flows Pertinent to Turbomachine Aerodynamics", Lecture Series 1998-02, VKI, Bruxelles.

[2] Ubaldi, M., Zunino, P., Campora, U., and Ghiglione, A., 1996, "Detailed velocity and turbulence measurements of the profile boundary layer in a large scale turbine cascade", ASME Paper No. 96-GT-42.

[3] Chen, W. L., and Leschziner, M. A., 1999, "Modeling turbomachine-blade flows with non-linear eddy-viscosity models and second-moment closure", Third European Conference on Turbomachinery - Volume A, IMechE Conference Transaction.

[4] Magagnato, F., 1999, "Unsteady flow past a turbine blade using non-linear two-equation turbulence models",

$\text{Re}_{2c} = 1600000$ and $\text{Re}_{2c} = 590000$ providing that the free stream turbulence intensity was the same for both the experiments. The integral parameters distributions show that the boundary layer development and also the transition process are greatly influenced by Reynolds number.

At the larger Reynolds number the transition begins earlier and is more gradual. Integral parameters suggest that transition occurs within 0.3 and 0.6 s/s_{max}.

At the lower Reynolds number the transition is very short and the boundary layer remains in laminar state until $s/s_{max} = 0.55$. Before this position both d^* and H_{12} show a steep increase, which indicates the tendency of the boundary layer to separation. At $s/s_{max} = 0.55$ suddenly both d^* and H_{12} fall down towards turbulent values and within a portion of approximately 0.15 of the surface length, the transition is completed.

According to Mayle and Schulz [18], from a practical standpoint the transition may be considered to begin where the skin friction coefficient deviates from the laminar values. For the present experiments the C_f distributions confirm the locations of transition beginning previously identified by other methods, but it comes out that the rms increase or the skewness variation are more sensitive indicators of the position where the transition begins.

Third European Conference on Turbomachinery - Volume A, IMechE Conference Transaction.

[5]   O'Donnell, F. K., and Davies, M.R.D., 2000, "Turbine Blade Entropy Generation Rate. Part II: The Measured Loss", ASME Paper No. 2000-GT-266.

[6]   Sieverding, C. H., Cicatelli, G., Desse, J.M., Meinke, M., and Zunino, P., 1999, *Experimental and Numerical Investigation of Time Varying Wakes behind Turbine Blades,* Vieweg, Braunschweig.

[7]   Cicatelli, G., and Sieverding, C.H., 1996, "The Effect of Vortex Shedding on the Unsteady Pressure Distribution Around the Trailing Edge of a Turbine Blade", ASME Paper No. 96-GT-359.

[8]   Durst, F., Kikura, H., Lekakis, I., and Jovanovic, J., Ye, Q., 1996, "Wall shear stress determination from near-wall mean velocity data in turbulent pipe and channel flows", *Experiments in Fluids*, no. 20, pp. 417-428.

[9]   Karpuk, M., and Tiederman, W., 1976, "Effect of Finite-Size Probe Volume upon Laser Doppler Anemometer Measurements", *AIAA Journal*, vol. 14, no. 8.

[10]   Durst, F., Martinuzzi, R., Sender, J., and Thevenin, D., 1992, "LDA-Measurements of Mean Velocity, RMS-Values and Higher Order Moments of Turbulence Intensity Fluctuations in Flow Fields with Strong Velocity Gradients", *6th Symposium on Applications of Laser Techniques to Fluid Mechanics*, Lisbon.

[11]   White, F. M., 1991, *Viscous Fluid Flow*, McGraw-Hill, Singapore.

[12]   Klebanoff, P. S., 1955, "Characteristics of Turbulence in a Boundary Layer with Zero Pressure Gradient", NACA Report 1247.

[13]   Halsted, D.E., Wisler, D.C., Okiishi, T.H., Walker, G.J., Hodson, H. P., and Shin H.-W., 1997, "Boundary Layer Development in Axial Compressors and Turbines: Part 3 of 4 - LP Turbines", *ASME Journal of Turbomachinery*, vol. 119, pp. 225-237.

[14]   Haueisen, V., Schröder, T., and Hennecke, D. K., 1997, "Measurements with Surface Mounted Hot-Film Sensors on Boundary Layer Transition in Wake Disturbed Flow", AGARD CP- 598, pp. 38-1, 38-14.

[15]   Romano, G. P., 1998, "The Measurements of Structure Functions with Laser Doppler Anemometry", *Ninth International Symposium on Application of Laser Anemometry to Fluid Dynamics*, Lisbon.

[16]   Benedict, L. H., Nobach, H., and Tropea, C., 1998, "Benchmark Tests for the Estimation of Power Spectra from LDA Signals", *Ninth International Symposium on Application of Laser Anemometry to Fluid Dynamics*, Lisbon.

[17]   Adrian, R.J., and Yao, C.S., 1987, "Power spectra of fluid velocities measured by laser Doppler velocimetry, *Experiments in Fluids*, vol. 5, pp. 17-28.

[18]   Mayle, R.E., and Schulz, A., 1996, "The Path to Predicting Bypass Transition", ASME Paper No. 96-GT-199.

[19]   Mayle R. E., 1991, "The Role of Laminar-Turbulent Transition in Gas Turbine Engines", ASME *Journal of Turbomachinery*, vol. 113, pp. 509-531.

[20]   Hourmouziadis, J., 1989, "Aerodynamic Design of Low Pressure Turbines", AGARD Lecture Series, No. 167.